

Different Electrochemical Behavior of Complexes Having the Identical Nitroso Ligand in *cis*-[Ru(N,O-hia)(bpy)₂]⁺ and *cis*-[Ru(N,O-hia)(bpy)(py)₂]⁺ (hia: Hydroxyiminoacetylacetonato, CH₃COC(NO)COCH₃[−])

Dai Ooyama, Noriharu Nagao,[#] Hiroshi Kuroda, Utako Satoh, F. Scott Howell, Masao Mukaida,^{*} Hiroataka Nagao,^{†, ##} and Koji Tanaka[†]

Department of Chemistry, Faculty of Science and Engineering, Sophia University, Kioi-cho 7-1, Chiyoda-ku, Tokyo, 102

[†]Institute for Molecular Science, Myodaiji, Aichi 444

(Received February 20, 1996)

[Ru(N,O-hia)(bpy)₂]⁺ (**I**) and [Ru(N,O-hia)(bpy)(py)₂]⁺ (**II**) (hia: CH₃COC(NO)COCH₃[−]) were prepared by the reactions of *cis*-[Ru(NO)(OH₂)(bpy)₂]³⁺ and *cis*-[Ru(NO)(OH)(bpy)(py)₂]²⁺ with acetylacetonate (Hacac) respectively. An X-ray structure analysis shows that the products have the identical nitroso ligand. Electrochemical behaviors of the complexes differ dramatically: **I** underwent an ECEC reaction, which could be illustrated as involving a structural rearrangement of the Ru-hia bonding, but **II** did not show such behavior and a typical reversible one-electron redox nature was found.

There has been growing interest in steric rearrangement accompanying an electron transfer reaction.¹⁾ A redox-induced nitro–nitrito linkage isomerization of the nitro complex of Ru(II) reported previously is one such example,²⁾ in which the corresponding nitrito complex of Ru(III) is generated. Detailed investigation of the electrochemical behavior has indicated that the nitrito species is capable of returning to the original nitro species via a one-electron redox process, though experimental conditions are limited to low temperatures (−40 °C).²⁾ Assuming some similarity between the nitro (−NO(O)) and nitroso (−NO(R)) moieties in their ligand behavior (since both have a NO moiety which can donate by the nitrogen atom, with a multiple bonding character), such a rearrangement is expected to occur in the nitroso complex of Ru(II). This appears to be the case. We found that [Ru(N,O-hia)(bpy)₂]⁺ (**I**) (hia: hydroxyiminoacetylacetonato, CH₃COC(NO)COCH₃[−]) showed a behavior which was understandable in terms of a nitro–nitrito like reversible rearrangement.²⁾ Strangely enough, the nitro–nitrito like reversible rearrangement was not observed in [Ru(N,O-hia)(bpy)(py)₂]⁺ (**II**), analogues to **I**: their skeletal fragments are different each other; “Ru(bpy)₂” for **I** and “Ru(bpy)(py)₂” for **II**. The present paper deals with syntheses, structures, and the characteristics of the complexes having the identical nitroso ligand.

Experimental

Materials and Measurements. *cis*-[Ru(NO)(OH₂)(bpy)₂]-

[#]Present address: Department of Chemistry, Stanford University (U.S.A.).

^{##}Present address: Department of Chemistry, Sophia University.

(PF₆)₃ and *cis*-[Ru(NO)(OH)(bpy)(py)₂](PF₆)₂ were prepared by modified literature procedures.^{3,4)} Elemental analyses and measurements of cyclic voltammetry, UV-vis, IR, and ¹H and ¹³C NMR spectra were carried out as reported previously.⁵⁾

Synthesis of *cis*-[Ru(N,O-hia)(bpy)₂](PF₆)₃·3H₂O (I**).** To a MeOH–H₂O (1 : 1) solution of *cis*-[Ru(NO)(OH₂)(bpy)₂](PF₆)₃ (100 mg/20 cm³) was added Hacac (1 cm³). The solution color changed immediately from brown to dark red. The solution was stirred at room temperature for 5–6 h. After filtration, the volume of the solution was reduced to 5–10 cm³, using a rotary evaporator, to precipitate dark-brown crystals. The product was purified by chromatography (Al₂O₃–CH₃CN). The solid material was collected, washed with cold water and ethanol, and finally with ether, and then air-dried. Yield 50 mg, 60%. Found: C, 40.47; N, 9.42; H, 3.52%. Calcd for C₂₅H₂₈N₅O₆PF₆Ru: C, 40.54; N, 9.46; H, 3.81%. Diamagnetic. ¹H NMR (CD₃CN): Assignments were difficult, but integration data indicate the existence of 22 protons per molecule. ¹³C NMR (CD₃CN) 22 resonances were detected (25 resonances were expected to the formula) δ = 204.26, 192.13, 160.85, 158.38, 158.36, 157.82, 156.51, 152.89, 152.26, 152.16, 139.19, 139.04, 137.59, 128.99, 128.38, 127.85, 127.24, 124.83, 124.52, 124.29, 31.75, 27.08. UV-vis (λ/nm (ε/dm³ mol^{−1} cm^{−1}) in CH₃CN) 287 (6.4 × 10⁴), 460 (1.6 × 10⁴). Synthesis of the complex has been reported, but it was characterized as *cis*-[Ru(hia)(H₂O)(bpy)₂]⁺ with an unidentate hia ligand,^{6a)} based on very limited data.

Synthesis of *cis*-[Ru(N,O-hia)(bpy)(py)₂](PF₆)₂ (II**).** The complex was prepared by exactly the same procedure as that described in the preparation of *cis*-[Ru(N,O-hia)(bpy)₂](PF₆)₃·3H₂O (**I**), except that a color change occurred when pH of the mixed solution of *cis*-[Ru(NO)(OH)(bpy)(py)₂](PF₆)₂ (75 mg/10 cm³) and Hacac (1 cm³) was adjusted to 4.5–7.0, using NaOH (1.0 mol dm^{−3}). Yield 50 mg, 70%. Found: C, 43.37; N, 10.12; H, 3.48%. Calcd for C₂₅H₂₄N₅O₃PF₆Ru: C, 43.61; N, 10.17; H, 3.51%. Diamagnetic. ¹H NMR (CD₃CN) Assignments were difficult, but inte-

gration data indicate the existence of 24 protons per molecule. ^{13}C NMR (CD_3CN) 18 resonances were detected (18 resonances were expected to the formula) $\delta = 204.79, 192.48, 162.43, 159.52, 158.40, 157.25, 153.29, 152.99, 140.41, 138.82, 138.39, 128.67, 128.07, 126.30, 123.99, 123.81, 31.37, 26.85$. UV-vis (λ/nm ($\epsilon/\text{dm}^3 \text{mol}^{-1} \text{cm}^{-1}$) in CH_3CN) 295 (2.4×10^4), 333 (1.5×10^4), 507 (1.2×10^4).

X-Ray Structure Determination. Crystallographic and intensity collection data of both **I** and **II** are summarized in Table 1. All the calculations were carried out on a Silicon Graphics Indy (for **I**) and Indigo (for **II**) Computer Systems, using TEXSAN program (for both **I** and **II**). The structures of **I** and **II** were solved by Patterson method and Direct method, respectively. Non-hydrogen atoms were refined anisotropically. Hydrogen atoms were placed in idealized positions and included in the structure factor calculations. Tables of the atomic coordinates, thermal parameters, bond lengths, and angles for the complexes have been deposited as Document No. 69036 at the Office of the Editor of Bull. Chem. Soc. Jpn.

Results and Discussion

$\{\text{MNO}\}^6$ -type nitrosyl complex acts as an electrophile toward ketones to give the complex with a nitroso ligand.^{6,7} Despite much work on this nitrosyl reactivity, only a few example of the structurally clarified products has been reported.⁸⁾

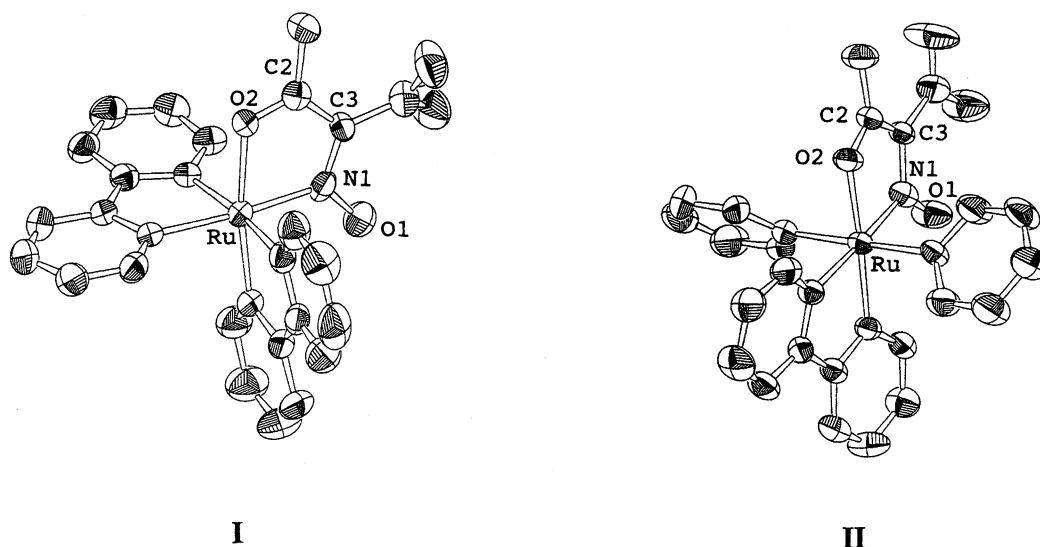
In the present work, a nitroso ligand formation occurred when nitrosyl complexes react with acetylacetone, either in *cis*- $[\text{Ru}(\text{NO})(\text{OH}_2)(\text{bpy})_2]^{3+}$ or *cis*- $[\text{Ru}(\text{NO})(\text{OH})(\text{bpy})(\text{py})_2]^{2+}$. An X-ray structural study established that their products, characterized as *cis*- $[\text{Ru}(\text{N},\text{O-hia})(\text{bpy})_2]^+$ (**I**) and *cis*- $[\text{Ru}(\text{N},\text{O-hia})(\text{bpy})(\text{py})_2]^+$ (**II**), contain the same form of hydroxyiminoacetylacetonato-N,O ligand. IR measurement showed bands which were tentatively assigned to νNO (or νCN) of the hia ligand at 1357 cm^{-1} (for **I**) and 1343 cm^{-1} (for **II**) (1333 cm^{-1} (for **I**) and 1332 cm^{-1} (for **II**) respectively in each ^{15}N labelled compounds), instead of νNO of the original nitrosyl moiety in the starting materials. The shifted value by the ^{15}N isotopic substitution is consistent with those of other labeling studies.^{8b)} Both nitroso complexes showed diamagnetic property.

1. Structure. ORTEP drawings of **I** and **II** are shown in Fig. 1. Their selected interatomic distances and angles are tabulated in Tables 2 and 3. Both cations have the expected octahedral coordination geometries, with a chelating hia ligand; the ligand can be regarded to be the combined species of the NO^+ cation and the di-anion of Hacac, through their nitrosyl nitrogen and methylene carbon atoms. Complex **I** is composed of one hia and two bpy ligand(s), with *cis*-type

Table 1. Summary of Crystal Data, Intensity Collection, and Structural Refinement of **I** and **II**

Crystal data		
Compound	$[\text{Ru}(\text{hia})(\text{bpy})_2]\text{PF}_6$ (I)	$[\text{Ru}(\text{hia})(\text{bpy})(\text{py})_2]\text{PF}_6$ (II)
Empirical formula	$\text{RuPF}_6\text{O}_3\text{N}_5\text{C}_{25}\text{H}_{22}$	$\text{RuPF}_6\text{O}_3\text{N}_5\text{C}_{25}\text{H}_{24}$
Formula weight	686.51	688.53
Crystal system	Monoclinic	Orthorhombic
Space group	$P2_1/n$	$Pbca$
$a/\text{\AA}$	12.218(2)	14.953(1)
$b/\text{\AA}$	15.085(3)	16.004(4)
$c/\text{\AA}$	15.055(2)	23.353(4)
$\beta/^\circ$	100.20(1)	
$V/\text{\AA}^3$	2730.8(7)	5588(1)
Z	4	8
$D_{\text{calc}}/\text{g cm}^{-3}$	1.670	1.636
Data collection		
Diffractionmeter	Rigaku AFC5S	Enraf-Nonius CAD4
Radiation	$\text{Mo K}\alpha$	$\text{Mo K}\alpha$
Wavelength/ \AA	0.71069	0.71069
Temperature/K	296	293
Crystal size/mm	$0.34 \times 0.22 \times 0.25$	$0.30 \times 0.20 \times 0.08$
Data collection mode	$\omega - 2\theta$	ω
$2\theta_{\text{max}}/^\circ$	55.0	49.9
Reflections collected	6516	5430
Independent reflections	3528	2457
Corrections	Lorentz-polarization Absorption (trans. factors: 0.9036-1.0251)	Lorentz-polarization Absorption (trans. factors: 0.9350-1.0332)
$F(000)$	1376	2768
Structural analysis and refinement		
Solution by	Patterson methods	Direct methods
Method of refinement	Full-matrix least-squares	Full-matrix least-squares
Final R indices ^{a)} [$I > 3\sigma(I)$]	$R=0.040, R_w=0.025$	$R=0.039, R_w=0.034$

a) $R = \sum ||F_o| - |F_c|| / \sum |F_o|$, $R_w = (\sum_w (|F_o| - |F_c|)^2 / \sum_w F_o^2)^{1/2}$.

Fig. 1. ORTEPs of *cis*-[Ru(hia)(bpy)₂](PF₆) (**I**) and *cis*-[Ru(hia)(bpy)(py)₂](PF₆) (**II**).Table 2. Selected Interatomic Distances (Å) for **I** and **II**

<i>cis</i> -[Ru(hia)(bpy) ₂](PF ₆) (I)	<i>cis</i> -[Ru(hia)(bpy)(py) ₂](PF ₆) (II)
Ru–N1	1.967(4)
Ru–O2	2.071(3)
N1–O1	1.254(4)
N1–C3	1.373(5)
O2–C2	1.268(5)
C2–C3	1.406(6)

Table 3. Selected Interatomic Angles (°) for **I** and **II**

<i>cis</i> -[Ru(hia)(bpy) ₂](PF ₆) (I)	<i>cis</i> -[Ru(hia)(bpy)(py) ₂](PF ₆) (II)
Ru–N1–O1	125.3(3)
Ru–N1–C3	115.3(3)
Ru–O2–C2	112.2(3)
O2–C2–C3	119.9(4)
N1–Ru–O2	79.4(1)
C2–C3–N1	113.0(4)

configuration, while **II** has the hia and bpy ligands in the equatorial positions and two pyridines in the axial positions. Differences of the bond distances and angles of the ligands between **I** and **II**, including those of the Ru–hia bonding (Ru–N and Ru–C), are relatively small (Tables 2 and 3), except for the results described below: the Ru–O distance in **I** is longer considerably than that of **II**. Contrastively, the N–C distance of hia in **I** is shorter than that of **II**. Other parameters of the hia ligand in both complexes are essentially the same. Although the X-ray structural study established that both complexes have the identical hydroxyiminoacetylacetonato ligand, their electrochemical behavior dramatically differs, as given below.

2. Electrochemical Behavior. Cyclic voltammograms of *cis*-[Ru(N,O-hia)(bpy)₂]⁺ (**I**) in CH₃CN at 25 °C, with 0.1 M TEAP (Tetraethylammonium perchlorate) as support-

ing electrolyte (1 M = 1 mol dm^{−3}), are shown in Fig. 2. A well-defined anodic wave ($E_{pa} = 0.98$ V vs. Ag|AgNO₃) was found, together with the coupled cathodic wave of the reverse scan in [Ru(N,O-hia)(bpy)₂]^{2+ / +}. The electron transfer process is diffusion-controlled with $i_{pa}/v^{1/2}$ constant over the range of scan rate used. The peak current ratio i_{pc}/i_{pa} is nearly unity and potential separations $\Delta E = E_{pa} - E_{pc}$ (0.98–0.91) = 70 mV of the anodic and cathodic waves correspond to the expected values for a one-electron reversible electrochemical couple. The peak separation is larger than the ideal Nernstian value of 59 mV, but is the value observed for various complexes of Ru(II).⁹ Another small cathodic wave appeared at 0.48 V (the wave was absent when the oxidative scan was returned near to 0.8 V), while the wave could not be detected when the experiment was carried out at low temperature (−40 °C), and only the coupled wave of [Ru(N,O-hia)(bpy)₂]^{2+ / +} appeared at 0.9–1.0 V.

An oxidative controlled-potential coulometry of **I**, carried out 1.1 V vs. Ag|AgNO₃ at 25 °C, showed that a reduction peak coupled with the corresponding oxidation peak appeared at 0.51 V ($E_{1/2}$) (Fig. 3-(a)). The coupled wave developed gradually with the progress of electrolysis, and only the wave was found at the final stage of the electrode reaction (Fig. 3-(b)). One mole of electrons per mole of the complex ($n = 1.0 \pm 0.06$) was confirmed to release for the oxidation. We attempted subsequently the reductive controlled-potential coulometry to the oxidized solution; the original coupled wave ($E_{1/2} = 0.95$ V) developed again when almost the same amount of electricity was consumed, showing the quantitative re-generation of the initial species, **I**.

The sequence of the electrode reaction can best be explained by a “square scheme” (ECEC mechanism),^{1,10} in which the oxidation and re-reduction of the complex occur via two separate reversible electron-transfer steps (Eqs. 1 and 2), each of which is coupled to the following reaction schemes:

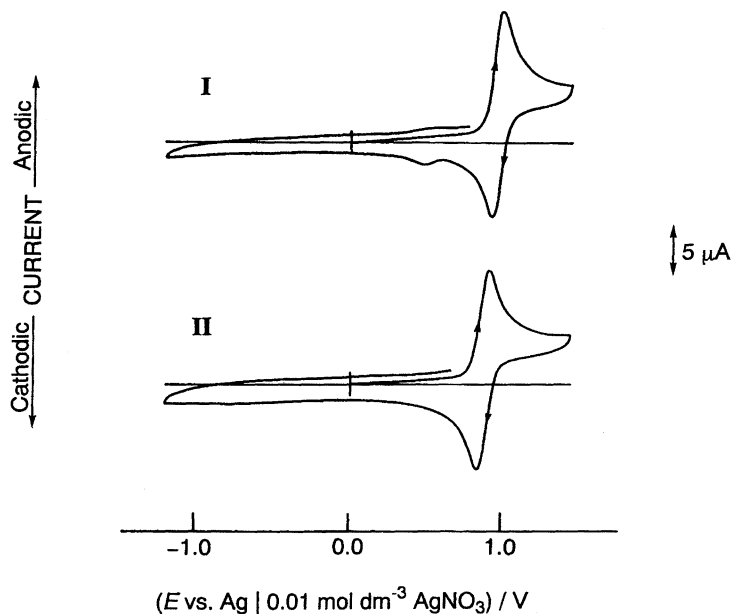
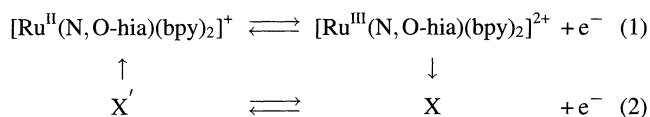


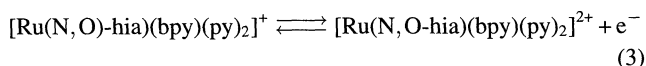
Fig. 2. Typical cyclic voltammograms of *cis*-[Ru(hia)(bpy)₂](PF₆) (I) (1.0×10^{-3} mol dm⁻³) and *cis*-[Ru(hia)(bpy)(py)₂](PF₆) (II) (1.0×10^{-3} mol dm⁻³) in CH₃CN at 25 °C (200 mV s⁻¹) (stationary Pt electrode, Et₄NClO₄ (0.1 mol dm⁻³)).



Such electrochemical behavior described in Eqs. 1 and 2 was not found in *cis*-[Ru(N,O-hia)(bpy)(py)₂]⁺ (II).

Cyclic voltammograms of *cis*-[Ru(N,O-hia)(bpy)(py)₂]⁺

(II) in CH₃CN at 25 °C, with 0.1 M TEAP as supporting electrolyte, are shown in Fig. 2. In the potential range -1.2 to +1.4 V, only one oxidation wave at a peak-potential difference, $|E_{\text{pa}} - E_{\text{pc}}|$ (0.91–0.84 V vs. Ag|AgNO₃), of ca. 70 mV is observed. Plots of peak currents vs. the square root of the scan rate are linear, indicating that diffusion-controlled redox processes are occurring at the electrode. The ratio of cathodic to anodic peak current, $i_{\text{pc}}/i_{\text{pa}}$, for Ru(III)/Ru(II) redox couple is near unity and independent of the scan rate 50–200 mV s⁻¹. We assign this process to a reversible one-electron oxidation–reduction expressed by Eq. 3.



The reversible one-electron nature of II could also be confirmed by a controlled-potential coulometry carried out at 5 °C:¹¹⁾ Exhaust oxidative electrolysis at a potential on the diffusion-limited plateau for the wave (1.0 V vs. Ag|AgNO₃) gave a value of $n=0.99$, and both cyclic and hydrodynamic voltammograms of the electrolyzed solution indicated the quantitative conversion to [Ru(N,O-hia)(bpy)(py)₂]²⁺. The return reduction of the generated species gave the original nitroso species with almost the same n value.

3. Structural Rearrangement Proposed for the One-Electron Redox Process of *cis*-[Ru(N,O-hia)(bpy)₂]⁺ (I).

A redox induced nitro-nitrito linkage isomerization of the complex coordinated nitro ligand has been investigated first by Meyer et al.,^{2a,2b)} followed by the present authors (H. N. and M. M.),^{2c,2d)} using *cis*-[Ru(NO₂)Cl(bpy)₂] and *trans*-[Ru(NO₂)Cl(py)₄] respectively. Although the final reaction product differs depending on the starting material used, both groups have reported essentially the same results: A one-electron oxidation of the nitro species of Ru(II) results in the generation of the corresponding nitrito species of Ru(III), which is capable of being returned to the original nitro species

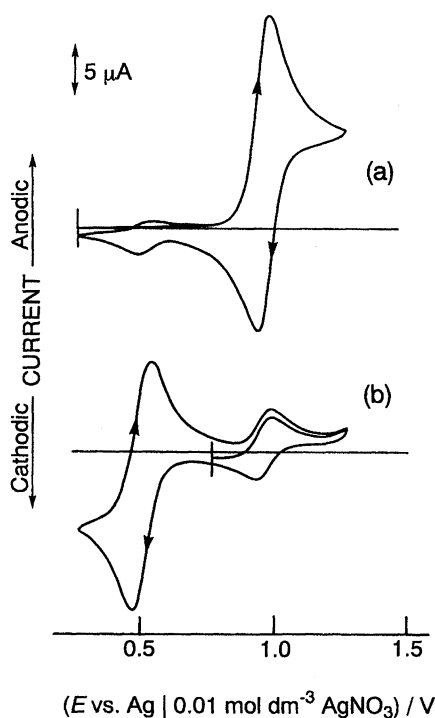


Fig. 3. Controlled-potential electrolysis of *cis*-[Ru(hia)(bpy)₂](PF₆) (I) in CH₃CN at 25 °C (200 mV s⁻¹). (a) CV prior to electrolysis; (b) CV of the electrolyzed solution ($n=0.92$).

by a one-electron reduction. The redox-induced rearrangement was explainable based on the ligand characteristics of the nitro moiety, which behaves as either the σ -donor or the π -acceptor. As the π -bonding nature between nitro ligand and metal is reduced when the formal oxidation state of a central metal increases, the Ru–N(nitro) bond is weakened and thus an electron-rich oxygen atom will come to prefer to bind with the higher-valent form of the Ru atom.^{2e)}

Assuming some similarity between the nitro (–NO(O)) and nitroso (–NO(R)) moieties, since both have a NO group which can donate with a multiple bonding character by the nitrogen atom, a similar redox-induced rearrangement is expected to occur in the nitroso complex of Ru(II), while we were not able to find such behavior in *cis*-[Ru(N,O-hia)(bpy)(py)₂]⁺ (II). No structural rearrangement has been reported in *cis*-[RuCl₂(bpy)₂] and *cis*-[RuCl₂(bpy)(py)₂]^{4,12)} they have either “(bpy)₂” fragment or “(bpy)(py)₂”, but lack a nitroso ligand.

We assume that a one-electron oxidation of I generates *cis*-[Ru^{III}(N,O-hia)(bpy)₂]²⁺ which results in a structural rearrangement to give *cis*-[Ru^{III}(O,O'-hia)(bpy)₂]²⁺ having a bidentate hia ligand (case (i) in Fig. 4: X species of Eq. 2). The rearranged species can be reduced to *cis*-[Ru^{II}(O,O'-hia)(bpy)₂]⁺ (X' species in Eq. 2), but the reduction is followed again by a structural rearrangement to return to the original species, complex (I).

The electrode reactions of both complexes (I and II) containing the identical nitroso ligand can be summarized in the scheme as written below (Fig. 5. In this scheme, only the three atoms of hia ligand that coordinate to ruthenium atom

are indicated, for clarity). A relatively fast rearrangement occurs, at 25 °C, in the {Ru(N,O-hia)} moiety of *cis*-[Ru^{III}(N,O-hia)(bpy)₂]²⁺ (I': the one-electron oxidation species of I), while such a rearrangement can not be found in *cis*-[Ru^{III}(N,O-hia)(bpy)(py)₂]²⁺ (II': the one-electron oxidation species of II): under the same conditions, the latter species undergoes a decomposition to give an electroinactive species, instead of the expected rearrangement. Clearly, $k_{\text{iso,III}}$ value of I' is larger than that of II' in a qualitative sense, while k_{decomp} value of I' is very small. Presently, no any information is available on $k_{\text{iso,II}}$ value.

In addition to the case (i) in Fig. 4, in which we assumed occurring the rearrangement of *cis*-[Ru(N,O-hia)(bpy)₂]⁺ (I) to give *cis*-[Ru(O,O'-hia)(bpy)₂]²⁺ (from the complex having a five membered-chelate hia ligand to the complex with a six membered one), two other cases (ii) or (iii) in Fig. 4) may also be considered as one possibility of the rearranged species. Case (ii) illustrates the complex with a O-bound unidentate hia ligand, *cis*-[Ru(O-hia)(solv)(bpy)₂]²⁺, and case (iii) shows the complex with a N-bound unidentate hia ligand, *cis*-[Ru(N-hia)(solv)(bpy)₂]²⁺. We imagine, however, that the explanation by the formation of these two species is rather difficult from the reversibility observed above, although their generation could not be ruled out.

Attempts were made to isolate a structurally isomerized species of I, in order to confirm the present assumption, using an equimolar amount of (NH₄)₂[Ce(NO₃)₆] as an oxidant, but we failed to obtain any pure product, because probably chemical instability of *cis*-[Ru(O,O'-hia)(bpy)₂]²⁺.

A problem remained why the present complexes showed

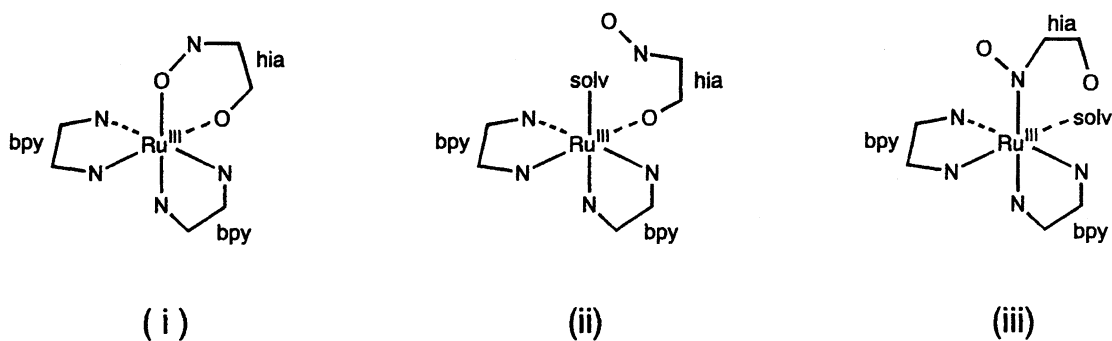


Fig. 4. Possible forms for the rearranged one-electron oxidation species of *cis*-[Ru(hia)(bpy)₂]⁺ (Only the three atoms of a hia ligand that coordinate to metals are indicated in this scheme, for clarity).

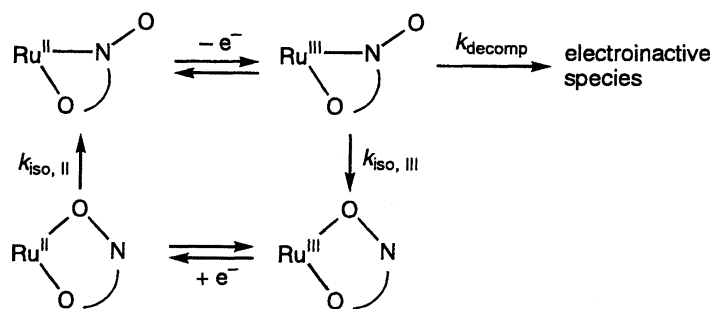


Fig. 5. Schematic illustration for the reaction processes.

the different redox behavior, even though both complexes have the identical nitroso ligand. At least two points ((a) and (b)) are important: Their skeletal fragments, "Ru(bpy)₂" (for **I**) and "Ru(bpy)(py)₂" (for **II**), are different either in (a) steric configurations or in (b) ligand compositions. Although we can not explain about the complex characteristics which would be produced by synergistic effects of both (a) and (b), a previous investigation has revealed the following results on the nitro–nitrito pairs of nitrosylruthenium(II), *cis*-[Ru(NO)(X)(bpy)₂]²⁺ and *cis*-[Ru(NO)(X)(bpy)(py)₂]²⁺ (X=NO₂, ONO).¹³ We found that a large different isomeric behavior was observable in their thermally-induced linkage isomerization: in *cis*-[Ru(NO)(X)(bpy)₂]²⁺, either the nitro isomer or the nitrito isomer underwent a rearrangement to gave an equilibrium mixture of both isomers. In *cis*-[Ru(NO)(X)(bpy)(py)₂]²⁺, however, only a nitro-to-nitrito rearrangement proceeded in *cis*-[Ru(NO)(NO₂)(bpy)(py)₂]²⁺. Any thermally-induced isomerization could not be found in the nitrito isomer, *cis*-[Ru(NO)(ONO)(bpy)(py)₂]²⁺. It is noted that skeletal fragments of these isomers of nitrosylruthenium(II) are corresponding to those of the present **I** and **II**.

We mention additionally that the present nitroso complex has been reported by other researchers without an X-ray structure determination,^{7c} *cis*-[Ru(bpy)₂(L)]⁺ (L=CH₃C(O)-C(NO)C(O)CH₃⁻): The structural description on 2,2'-bipyridine ligands of their complex, including the nitroso ligand, appears to be the same to that of **I**. However, their complex has shown a simple reversible one-electron nature as in the case of **II**: no ECEC mechanism was observed.

This work was supported by the Joint Studies Program (1993–1994, No. 5-655 and No. 6-258) of the Institute for Molecular Science.

References

- 1) a) W. E. Geiger, "Progress in Inorganic Chemistry," John Wiley, New York (1985), Vol. 33, pp. 275–351; b) D. H. Evans, *Chem. Rev.*, **90**, 739 (1990).
- 2) a) F. R. Keene, D. J. Salmon, J. L. Walsh, H. D. Abruna, and T. J. Meyer, *Inorg. Chem.*, **19**, 1896 (1980); b) H. D. Abruna, J. L. Walsh, T. J. Meyer, and R. W. Murry, *Inorg. Chem.*, **20**, 1481 (1981); c) H. Nagao, F. S. Howell, M. Mukaida, and H. Kakihana, *J. Chem. Soc., Chem. Commun.*, **1987**, 1618; d) H. Nagao, H. Nishimura, Y. Kitataka, F. S. Howell, M. Mukaida, and H. Kakihana, *Inorg. Chem.*, **29**, 1693 (1990); e) N. Nagao, H. Nagao, H. Nishimura, H. Kuroda, K. Satoh, F. S. Howell, and M. Mukaida, *Bull. Chem. Soc. Jpn.*, **66**, 1937 (1993); f) N. Nagao, D. Ooyama, K. Oomura, Y. Miura, F. S. Howell, and M. Mukaida, *Inorg. Chim. Acta*, **225**, 111 (1994).
- 3) S. A. Adeyemi, F. J. Miller, and T. J. Meyer, *Inorg. Chem.*, **11**, 994 (1972).
- 4) D. Ooyama, Y. Miura, Y. Kanazawa, F. S. Howell, N. Nagao, M. Mukaida, H. Nagao, and K. Tanaka, *Inorg. Chim. Acta*, **237**, 47 (1995).
- 5) H. Nagao, H. Nishimura, H. Funato, F. S. Howell, M. Mukaida, and H. Kakihana, *Inorg. Chem.*, **28**, 3955 (1989).
- 6) a) M. Mukaida, M. Yoneda, and T. Nomura, *Bull. Chem. Soc. Jpn.*, **50**, 3053 (1977); b) M. Mukaida, T. Nomura, and T. Ishimori, *Bull. Chem. Soc. Jpn.*, **48**, 1443 (1975).
- 7) a) J. H. Swinehart, *Coord. Chem. Rev.*, **2**, 385 (1967); b) K. Schug and C. P. Guengrich, *J. Am. Chem. Soc.*, **101**, 235, (1979); c) A. R. Chakravarty and A. Chakravarty, *J. Chem. Soc., Dalton Trans.*, **1982**, 1765; d) J. H. Swinehart and W. G. Schmidt, *Inorg. Chem.*, **2**, 232 (1967).
- 8) a) F. Bottomley, M. V. F. Brooks, D. E. Paéz, P. S. White, and M. Mukaida, *J. Chem. Soc., Dalton Trans.*, **1983**, 2465; b) F. Bottomley, P. S. White, M. Mukaida, K. Shimura, and H. Kakihana, *J. Chem. Soc., Dalton Trans.*, **1988**, 2965.
- 9) a) A. B. P. Lever, *Inorg. Chem.*, **29**, 1271 (1990), and the references cited therein; b) D. Ooyama, N. Nagao, F. S. Howell, M. Mukaida, H. Nagao, and K. Tanaka, *Bull. Chem. Soc. Jpn.*, **68**, 2897 (1995).
- 10) A. J. Bard and L. R. Faulner, "Electrochemical Methods Fundamentals and Applications," Wiley, New York (1980), pp. 222 and 452.
- 11) The experiment was carried out at 5 °C to avoid a decomposition of the one-electron oxidation species(*cis*-[Ru(N,O-hia)(bpy)(py)₂]²⁺): at 25 °C, the species underwent gradually a decomposition during the electrolysis, without showing an electrochemical behavior that was observed in *cis*-[Ru(N,O-hia)(bpy)₂]⁺ (**I**). (We have found that **I** shows the electrochemical behavior illustrated in Eqs. 1 and 2, even at –40 °C).
- 12) J. N. Braddock and T. J. Meyer, *Inorg. Chem.*, **12**, 723 (1973).
- 13) D. Ooyama, N. Nagao, H. Nagao, Y. Miura, A. Hasegawa, K. Ando, F. S. Howell, M. Mukaida, and K. Tanaka, *Inorg. Chem.*, **34**, 6024 (1995).